

Experience in Designing Autonomous Airplane

Róbert Schochmann, Jakub Pilka, Martin Suchý, Michal Kusenda

FEI STU Ilkovičova 3 812 19 Bratislava 1

www.animatechnika.com

robo@schochmann.com

pilka.jakub@gmail.com

13chaser.@gmail.com

Abstract: In this paper we present experience gathered in our work on UAV design. UAVs (Unmanned Autonomous, or Aerial Vehicles) are radio controlled flying vehicles, e.g. airplanes equipped with RF communication systems, cameras and sensors (e.g. accelerometers, gyros, temperature and pressure sensors, a GPS module etc.) enabling to be capable of autonomous flight. Currently UAVs are mostly used in the military area to safely watch areas of potential risk without endangering the lives of people otherwise needed to provide information on such areas. Lately UAVs have begun to make their way into civil applications as well. Possible uses include monitoring of forest fires, following fleeing suspects by the police, scanning of ground surface to create maps on a local level and so on, or simply for fun.

1. INTRODUCTION

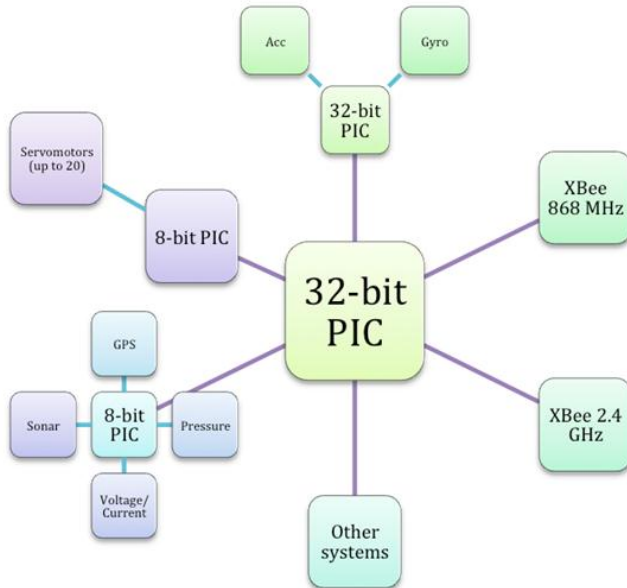
In this paper we present our achievements gain so far in approximately 3 year experience. Our goal is to design hardware and software architecture for a fully autonomous UAV capable of flying to its destination to carry out some task (e.g. to gather visual information) and safely returning without the need for user interference.

2. CONSTRUCTION AND ELECTRONICS

We chose a standard model RC (Remotely Controlled) plane made of balsa and plywood. This means that it is light but also strong enough to survive vibrations generated by the 4 horsepower, 2-stroke combustion engine. The total weight is around 4.5 kilograms (including electronics) and it is possible to add another 0.75 kilogram load and still maintain stable flight conditions.

The plane electronics is powered by two Li-Pol batteries (one for the main system and the other for the servomotors). The star architecture is centred around the main 32-bit PIC (Peripheral Interface Controller) microcontroller. Other 8-bit PICs whose purpose is to collect and process data from sensors are connected to it. The reason for this architecture is distribute the A/D conversion time, whereas the main μC can be used for other necessary calculations. The main advantage of this architecture is that the main μC can work without having to wait for its peripheral circuits to finish a conversion from the analogue sensors. Another advantage is the ease possibility of adding additional system components since the computing power of the main μC is never fully used. We prepared our PCB (Printed circuit board) designs to be able to add more electronic equipment if needed. XBee RF communication modules compliant with IEEE 802.11 standards are used for wireless communication with the model.

The control station is composed of a laptop, joystick to control the aircraft and of the XBee RF communication



module.

Fig. 1. Hardware star architecture

3. UTILITY SOFTWARE OF THE GROUND STATION

The utility software gives the pilot all the necessary information he needs to pilot the plane. This includes a video feed from the on-board camera, acceleration in X, Y and Z axes, roll and pitch indication is also present. Also the joystick calibration will be available, as well as the fuel level indication and battery charge status. Our goal is to make GUI as simple and intuitive as possible so that the pilot can fully concentrate on controlling the aircraft.

4. COMMUNICATION

Communication between ground station and the plane is performed via XBee RF modules at a 115 200 baud per sec. data rate. Communication runs on 868 MHz frequency. Each of the modules has its role in the network. One acts as coordinator (ground station), the other as end-device (plane). The coordinator works in a broadcast mode so it does not require acknowledgement messages from the end device since they are not needed because minor data dropouts are acceptable. This further increases communication speed. Before the network is established, the coordinator finds the most suitable channel and sets a PAN ID (Personal Area Network) specific only to this network. The end device then scans for coordinator networks and associates only with the one with a specific 64-bit address. This ensures no other coordinators interfere with our communication.

5. PRIMITIVE AUTOPILOT

From the GPS module we get the following data:

- Latitude
- Longitude

True course in degrees is calculated using the following formula:

$$c = \text{acos} \left(\frac{\sin(\text{Lat}2) - \sin(\text{Lat}1) * \cos(d)}{\cos(\text{Lat}1) * \sin(d)} \right)$$

Where 'Lat1' and 'Lat2' are gathered directly from the GPS module ('Lat1' being the last known latitude and 'Lat2' the current latitude value) and 'd' is the great circle distance. This is the shortest path between two points on a sphere, in our case the globe.

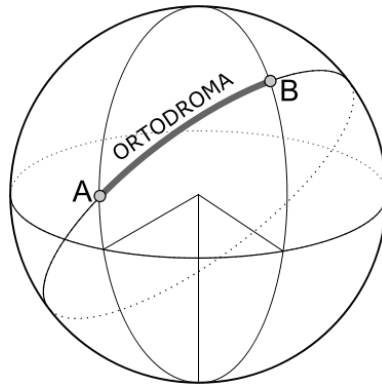


Fig. 2. Great circle distance

From the gathered data we can calculate out true heading. The waypoint heading is a constant telling the autopilot where to steer the aircraft.

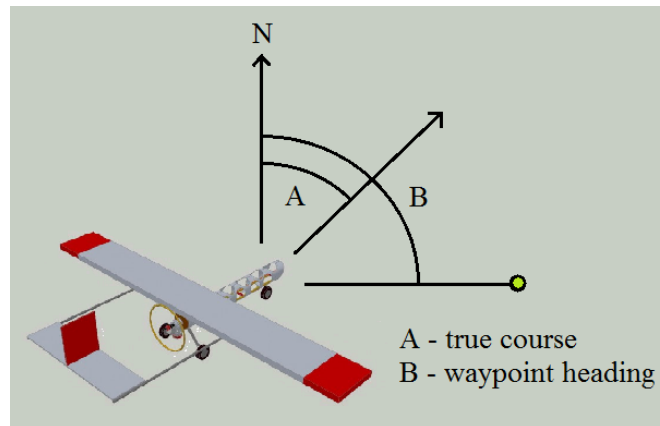


Fig. 3. Waypoint heading calculation

6. SENSORS

6.1 GPS module

Our GPS module has an RS-232 output with 4800 baud per sec. communication speed. The data refresh rate is 1 Hz. GPGGA is the protocol we use. The output data consists of 15 blocks, preceded by a synchronization symbol '\$', and a comma separating each data block. The data structure is:

\$GPGGA,hhmmss.ss,llll.ll,a,yyyy.yy,a,x,xx,x.x,x.x,M,x.x,M,x.x,xxxx*hh

- 1 = World time
- 2 = Latitude
- 3 = North/South
- 4 = Longitude
- 5 = East/West
- 6 = GPS signal quality indication
- 7 = Number of satellites
- 8 = Horizontal spacing
- 9 = Altitude (above sea level)
- 10 = Unit (meter)

- 11 = Altitude (geoid)
- 12 = Unit (meter)
- 13 = Time of last refresh
- 14 = ID#
- 15 = Checksum

6.2 Accelerometers and gyroscopes

To get values for pitch, roll and acceleration we use a CHAR6D module.



Fig. 4. CHR-6d module

The CHR-6d is a 6-axis IMU, combining three accelerometer axes and three rate gyro axes in a .8" by .7" footprint. An onboard ARM Cortex™ processor samples and filters gyro and accelerometer outputs and sends results over a TTL (3.3V) UART.

Data Outputs

- 3-axis roll rates (+/- 400 deg/s)
- 3-axis acceleration (+/- 3 g)
- Pitch and roll angles
- 16-bit effective measurement resolution (after oversampling and decimation)

Features

- Configurable digital filter (windowed Parks-McClellan FIR)
- Onboard EKF for pitch and roll angle estimation
- Automatic bias calibration
- High bias stability over temperature
- Adjustable output rates (20 Hz - 300 Hz)
- TTL (3.3V) UART interface

6.3 Ultrasound sonar

We added sonar oriented towards the ground to assist while landing because the camera mounted on top of the plane does not give information useful for landing. The sonar measurement range is circa up to 8 meters and its refresh rate is around 14 Hz.

6.4 Prandtl probe

To measure flight speed of aircraft Prandtl probes are used enabling to measure flow velocity of liquids, in our case plane velocity with respect to surrounding air. It is based on measuring difference between the total pressure and the static pressure of flow in a point of flow streamline. The velocity meter in central part of Prandtl probe flow velocity is brought to zero isentropically. With velocity equal to zero measured pressure equals to the total pressure. On outer part of probe where the flow streamlines are tangent the flow velocity is not changed and the pressure measured on that part is called the static pressure. The difference between the total and the static pressure in one point of flow streamline is called dynamic pressure. The dynamic pressure represents kinetic energy of the flow.

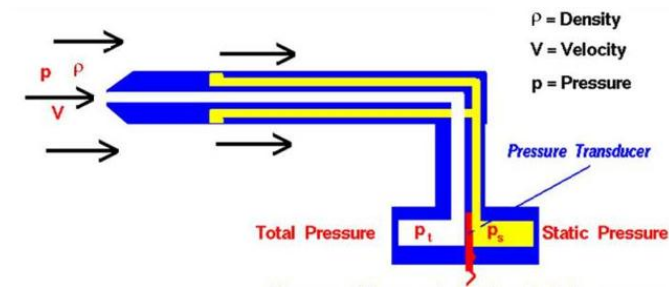


Fig. 5. Measurement principle

Flow velocity can then be calculated.

For ideal gas:
$$v = \sqrt{\frac{2(p_1 - p_2)}{\rho}}$$

For real airflow:

$$v = \sqrt{\frac{2k}{k-1} \cdot g \cdot R \cdot T \cdot \left(1 - \left(\frac{p_2}{p_1}\right)^{\frac{k-1}{k}}\right)}$$

These equations work only for speeds lower than the speed of sound what fully satisfies our application.

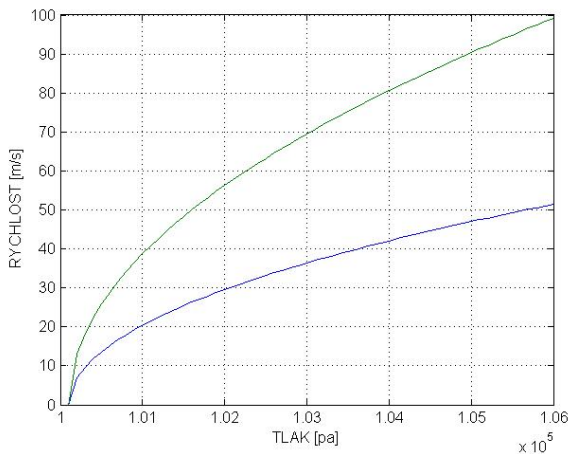


Fig. 6. Speed measurement characteristic for ideal gas (green) and real gas (blue)

The Prandtl probe is capable of measuring speeds up to 100 m/s. This means dynamic pressure up to 6 kPa. The most suitable pressure sensor to measure such values has proven to be MPXV4006G. This is a piezoresistive pressure sensor with integrated temperature compensation.

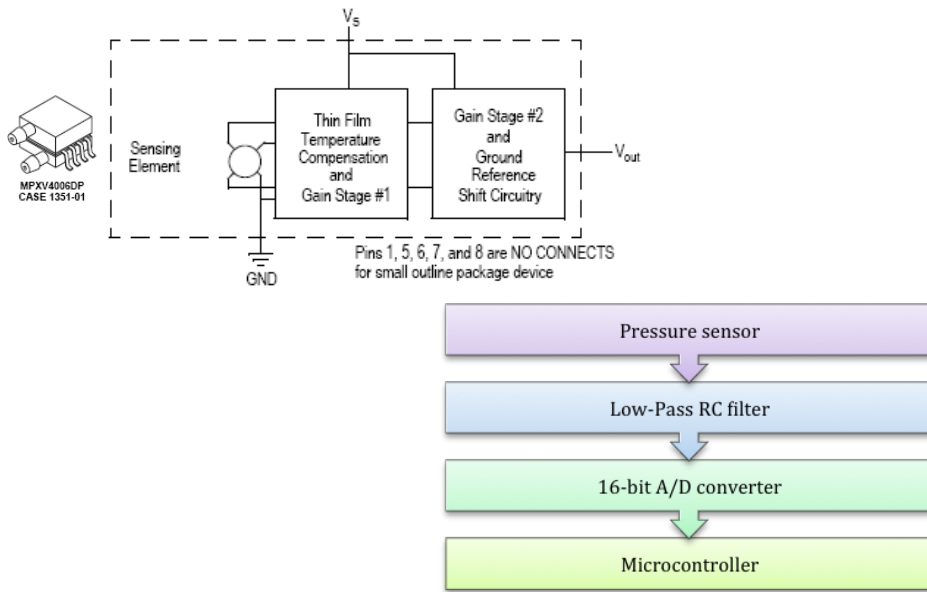


Fig. 7. MPXV4006DP pressure sensor diagram and case and module architecture

Sensor output is an analogue signal from 0.2 to 4.7 Volts. Thus, the measurement sensitivity is 766 mV/kPa. For a proper pressure measurement we needed to design appropriate filtering and A/D conversion.

7. PROBLEMS AND SOLUTIONS

7.1 Parachute

Since in the development of the flight control system one has to consider potential problems that could lead to serious malfunctions, the aeroplane should be equipped with a parachute safety system. In the case of uncontrolled movement it should automatically start its activity and to assure sufficiently damped landing.

Before choosing the appropriate type of parachute we need to put together some basic data. This includes:

- Max falling speed
- Weight of the plane + weight of the parachute itself
- Density of air
- Max limit for oscillation
- Deployment speed

There are two possible choices for the parachute shape. One is a more stable cross-chute and the other a cone-shaped chute that is more prone to oscillations but has a higher air resistance constant.



Fig. 8. Cross chute

Air resistance constant = (0.6 – 0.85)

Deployment force constant = (1.1 – 1.2)

Oscillation = $(0^\circ - \pm 3^\circ)$



Fig. 9. Our parachute

Air resistance constant = $(0.75 - 0.9)$

Deployment force constant = (1.8)

Oscillation = $(\pm 10^\circ - \pm 35^\circ)$

Equations needed:

- Brake force

- G-force

$$F_t = m * g = 44,15 \text{ N}$$

- Falling speed

$$v_D = \sqrt{\frac{2 * m * g}{A * C * \rho}} = 2,12 \text{ m s}^{-1}$$

- Surface area

$$A = \pi * r^2 = 5,3 \text{ m}^2$$

- Diameter after deployment

$$D = \sqrt{\frac{8 * m * g}{v_D^2 * \rho * C * \pi}} = 2,6 \text{ m}$$

Where:

- C – resistance constant

- ρ – air density

- g – gravitational force constant

The parachute test proved that our calculations were correct, at 5 m/s windspeed we measured a force of roughly about 50 Newtons. This means it is possible to use this parachute as a backup landing system in case of emergencies or lack of landing space.

7.2 Communication fault protection

In case of interrupt of communication, the plane could become a hazard for surroundings. To prevent such situations, if communication is interrupted, the flaps are extended to the maximum possible position so the plane is forced in a corkscrew motion sending it directly to the ground instead of flying off to a populated area. Also to prevent damage to the plane and/or injuries to anyone standing beneath the falling plane the safety parachute deploys after entering communication fault mode. This ensures a softer landing.

7.3 Vibrations problems

The most serious problem solved so far is caused by vibrations generated by the engine. These are detected by accelerometers and; in fact, they are so strong that it does not produce any relevant data. The problems are caused by a number of factors, which include:

- Combustion of fuel in the engine cylinder. Since the piston and everything connected to it have some momentum, combustion of fuel causes a force, which forces the engine in the opposite direction of piston movement. This is the cause of Z-axis vibrations.
- Rotation axis vibrations are caused by compression and decompression of gasses in the engine cylinder. This effect causes mild deceleration and acceleration of the propeller thus transferring force into the body of the plane.

The CHR6d module oversamples and decimates the ADC data on all channels to reduce quantization noise and increase the effective ADC resolution to 16 bits. After decimation, sensor data is processed using a configurable Parks-McClellan window FIR (Finite Impulse Response) low-pass filter. The corner frequency of the filter is independently adjustable for each channel from 10 Hz to 140 Hz in 10 Hz increments.

FIR (Finite Impulse Response) filters represent one of two primary types of digital filters used in Digital Signal Processing (DSP) applications. FIR filters sometimes have the disadvantage that they require more memory and/or calculation to achieve a given filter response characteristic. Also, certain responses are not practical to implement with FIR filters.

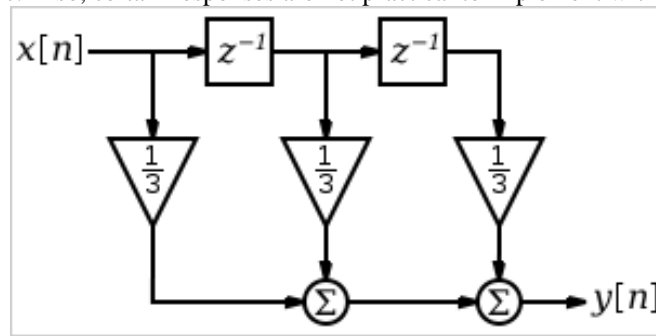


Fig. 10. Block diagram of a simple FIR filter

Tap - A FIR "tap" is simply a coefficient/delay pair. The number of FIR taps is an indication of:

- 1) The amount of memory required to implement the filter
- 2) The number of calculations required
- 3) The amount of "filtering" the filter can do

In effect, more taps means more stop band attenuation, less ripple, narrower filters, etc.

The measurement was done for idle thrust of the engine (25 rpm/ 25 Hz). The body of the plane was placed on a fixed, rigid base. During measurement we adjusted values of the low-pass filter and tap value. These values were set to 140Hz for the filter and 8 taps during the first part of measurements and 10Hz 64 taps for the second part.

There is a very noticeable reduction of interference after the second setting on both the accelerometers and gyros.

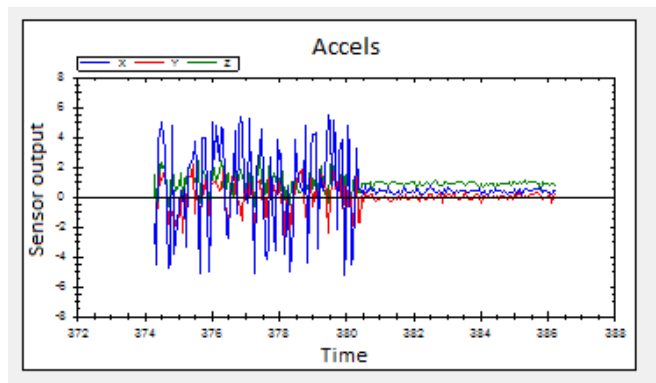


Fig. 21. Accelerometer measurement

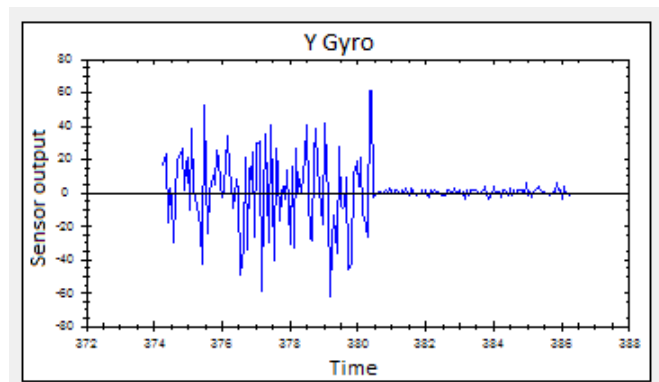


Fig. 32. Gyro measurement

Pitch and roll angles are calculated using an extended Kalman filter, which is a component of the sensor module. Even after filtration there is some interference. This can be caused by imperfection of the whole system (accumulated vibrations in the hull, irregular operation of the engine etc.).

The basic theory behind the filter is this: if the sensor is not accelerating, then the onboard accelerometers can be used to detect gravity and (hence) estimate pitch and roll angles. In general, however, the sensor might be moving around and vibrating, so that in the short term, the accelerometers can't be trusted. This is where the rate gyros come in. MEMS (Microelectromechanical systems) gyro output is angular velocity. In order to get pitch and roll angles we need to integrate this velocity. Since rate gyros are less sensitive to acceleration, they can be used to estimate changes in pitch and roll in the short term. But angle estimates produced by rate gyros tend to drift over time. The onboard Extended Kalman Filter is used to combine accelerometer and rate gyro measurements in a way that removes long-term drift, and that removes the negative effect of transient vibrations. In practice, a tradeoff must be made between trusting the rate gyros and trusting the accelerometers. When the filter trusts rate gyros more, it is less sensitive to acceleration and more sensitive to nonzero gyro biases. On the other hand, if the filter trusts accelerometers more, it is more sensitive to bad acceleration, and less sensitive to nonzero gyro biases.

To get the plane's absolute position we need to avoid long-term double integration of acceleration values (leading to increasing relative position value errors) by using acquired GPS position data in our calculations. By fusing this data together we get all the information about the plane's velocity and absolute and relative position we need.

On the CHR6d, the Extended Kalman Filter is tuned by adjusting the process variance. If the sensor were mounted on a rotorcraft, for example, the process variance could be set very low to reduce the effect of vibrations.

8. CONCLUSION

UAV development is directly tied with multiple disciplines; mathematics, physics, engineering, telecommunication, IT and many others. The project is conducted in order to achieve fully autonomous flight equipment with no input from humans. In proposing solutions, we note the aircraft hazard to people in case of errors.

We emphasize on the criterion of real-time, safety and transfer the event of failure on backup safety systems.

ACKNOWLEDGMENTS

The work has been partially supported by the grant agency VEGA-1/0656/09 Integration and development of nonlinear and robust control methods and their application to control of flying vehicles. This support is very gratefully acknowledged.

REFERENCES

- [1]<http://www.pipeflowcalculations.com/prandtl/>
- [2]<http://www.grc.nasa.gov/WWW/K-12/airplane/pitot.html>

[3] <http://www.dspguru.com/dsp/faqs/fir/basics>

[4] http://en.wikipedia.org/wiki/Finite_impulse_response

[5] http://www.pololu.com/file/0J342/chr6d_datasheet.pdf